ICSV13 - Vienna
The Thirteenth International Congress on Sound and Vibration
Vienna, Austria, July 2-6, 2006

ACOUSTIC WAVE SCATTERING FROM AN ENCASED CLAD ROD

Sina Sodagar*[1], Farhang Honarvar[1], and Anthony N. Sinclair[2]

[1]Faculty of Mechanical Engineering, K. N. Toosi University of Technology
P.O. Box 16765-3381, Tehran, Iran
[2]Department of Mechanical and Industrial Engineering, University of Toronto,
5 King's College Road, Toronto, Ontario M5S 3G8, Canada
ssodagar@alborz.kntu.ac.ir

Abstract

In this paper, a mathematical model for the scattering of a plane acoustic wave incident at an arbitrary angle on an encased isotropic clad rod is developed. The model is based on the normal-mode expansion method. The isotropic solid matrix around the cylinder precludes the appearance of the leaky Rayleigh modes that dominate the spectrum of an immersed cylinder. Instead, interfacial modes contributing to the scattered spectrum are observed. These modes could be instrumental in the development of ultrasonic nondestructive evaluation techniques for assessment of the matrix-fiber bonds in fiber reinforced composite materials. The presence of a solid matrix that supports shearing action leads to scattered compression and shear waves with polarization components in both the axial direction and $r-\theta$ plane. The model has been verified on various simpler cases, such as embedded solid cylinder and immersed clad rods. Work in underway to establish the conformity of the results with experimental data.

INTRODUCTION

The problem of scattering of obliquely incident waves from cylindrical objects is becoming more important due to increasing needs for ultrasonic nondestructive evaluation (NDE) of composites. In particular, the problem of acoustic wave scattering from multi-layered cylindrical components has been considered by a few researchers. Some studied wave scattering from multi-layered cylindrical shells, while others investigated multi-layered rods.

Elastic wave scattering from a cylindrical inclusion in a solid has been well documented in the literature [1-5]. Addison and Sinclair developed an analytical model for computing the diffraction spectrum and phase diagram of a plane compression wave incident on a long fiber embedded in a solid elastic matrix [5]. A comprehensive list of early publications can be found in Ref [5]. Huang *et al.* studied the scattering of waves from multilayered fibers and the effect of fiber-matrix interphasial properties [6-8]. Almost all previous studies address normal incidence of an elastic wave on a solid cylinder. White obtained general solutions for oblique elastic wave scattering from a cylinder but did not report numerical results [1]. White's solution was also summarized in some detail by Pao and Mao [3]. Experimental results on the scattering of elastic waves obliquely incident on a cylinder encased in a solid matrix with application to nondestructive evaluation of composites have been reported by Johnston *et al.* [9]. In 1996 Huang *et al.* extended their earlier theoretical work on the scattering of normally incident elastic waves from a multilayered cylinder to oblique scattering using a transfer matrix approach [10].
Honarvar and Sinclair used a normal-mode expansion based on decomposition of displacement field to calculate the scattered pressure field of an immersed transversely isotropic cylinder [11]. They also formulated the problem of scattering of an obliquely incident plane acoustic wave from an infinite solid elastic clad rod in 1997 [12]. In 2000 Fan used the formalism of Ref. [11] for modeling the scattering of waves from a transversely isotropic cylinder encased in an isotropic matrix [13].
In this paper, a mathematical model for the scattering of a plane acoustic wave incident at an arbitrary angle on an encased clad rod is developed.

FORMULATION OF THE PROBLEM

Consider a plane wave traveling through an infinite, isotropic medium, incident at an angle α on a long, encased isotropic clad rod of radius $r = a$, see Fig. 1. A cylindrical coordinate system (r, θ, z) is chosen with the z direction coincident with the axis of the cylinder.
The displacement field $\vec{u}(r, \theta, z, t)$ in the matrix can be expressed in terms of three scalar potentials ϕ, ψ and χ [11],

$$\vec{u} = \nabla\phi + \nabla\times(\chi\,\hat{e}_z) + a\ \nabla\times\nabla\times(\psi\,\hat{e}_z), \tag{1}$$

In the matrix material, each of the three wave potentials can have two components: an "incident" and a "scattered" wave component.
For the case where the incident wave is compressional with circular frequency ω, the associated normalized potential function in the matrix has the general form [6],

$$\phi_{3,incident} = \sum_{n=0}^{\infty} \varepsilon_n\,(i)^n J_n(K_{2\perp} r)\cos(n\theta)\exp(i[K_{2z} z - \omega t]), \tag{2}$$

where $K_{2\perp} = K_2 \cos\alpha$, $K_{2z} = K_2 \sin\alpha$, and K_2 is the compressional wave number in the matrix material.

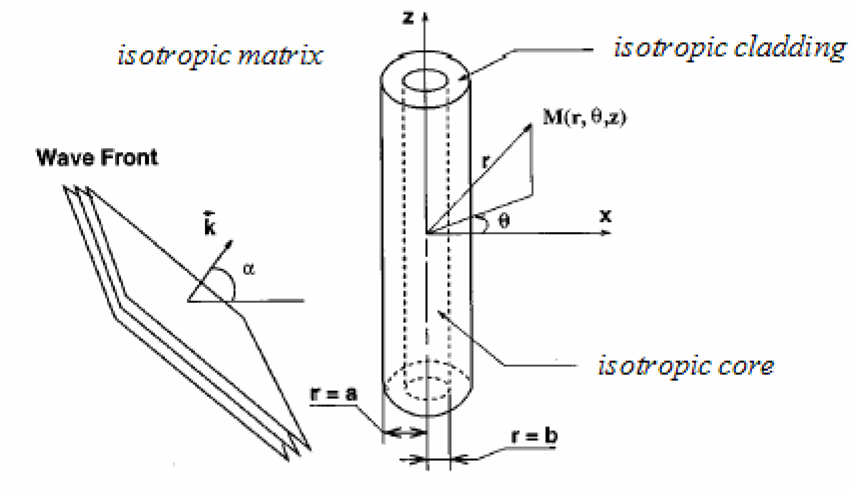

Fig. 1. Geometry of a plane wave obliquely incident on an encased clad rod.

The symbol ε_n is the Neumann factor ($\varepsilon_n = 1$ *for* $n = 0$, *and* $\varepsilon_n = 2$ *for* $n > 0$). The J_n terms are Bessel functions of the first kind. For the a shear wave polarized in the $r-\theta$ plane, the associated normalized potential is,

$$\chi_{3,incident} = \sum_{n=0}^{\infty} \varepsilon_n (i)^n J_n(k_{2\perp} r) \sin(n\theta) \exp(i[k_{2z} z - \omega t]), \tag{3}$$

where $k_{2\perp} = k_2 \cos\alpha$, $k_{2z} = k_2 \sin\alpha$, k_2 is the shear wave number in the matrix. Last, for the case of an incident shear wave polarized in the $r-z$ plane, the associated potential function is [14],

$$\psi_{3,incident} = \sum_{n=0}^{\infty} \varepsilon_n (i)^n J_n(k_{2\perp} r) \cos(n\theta) \exp(i[k_{2z} z - \omega t]). \tag{4}$$

Now consider the component of the displacement field $\vec{u}$ in the matrix material originating from waves scattered by the cylinder, and the associated potential functions [5],

$$\phi_{3,scattered} = \sum_{n=0}^{\infty} \varepsilon_n (i)^n P_n H_n(K_{2\perp} r) \cos(n\theta) \exp(i[\kappa_{2z} z - \omega t]), \tag{5}$$

$$\psi_{3,scattered} = \sum_{n=0}^{\infty} \varepsilon_n (i)^n R_n H_n(k_{2\perp} r) \cos(n\theta) \exp(i[\kappa_{2z} z - \omega t]), \tag{6}$$

$$\chi_{3,scattered} = \sum_{n=0}^{\infty} \varepsilon_n (i)^n S_n H_n(K_{2\perp} r)\sin(n\theta)\exp(i[\kappa_{2z} z - \omega t]), \tag{7}$$

where H_n represents the Hankel function of the first kind and P_n, R_n and S_n are unknown coefficients to be determined. The κ_{2z} can be either equal to K_{2z} or k_{2z} depending on the nature of the incident wave. The total displacement in material 3 can now be obtained by summing the incident and scattered components,

$$u_2 = u_{2,incident} + u_{2,scattered}, \tag{8}$$

and making the appropriate substitutions from Eqs. (1) – (7).

Isotropic Clad Rod

If the isotropic core and cladding media are designated by subscript $i = 1, 2$, respectively, then using Helmholtz displacement potential functions, ϕ_i (scalar) and ψ_i (vector), the Navier's equation for each medium can be written as

$$\nabla((\lambda_i + 2\mu_i)\nabla^2\phi_i - \rho_i \frac{\partial^2\phi_i}{\partial t^2}) + \nabla\times(\mu_i \nabla^2\psi_i - \rho_i \frac{\partial^2\psi_i}{\partial t^2}) = 0, \tag{9}$$

where λ_i and μ_i are the Lame constants and ρ_i are the material densities. By expanding Eq. (9), four partial differential equations in terms of potential functions are obtained for each medium. In order to satisfy these partial differential equations, the potential functions should be of the following forms [12],

$$\phi_1 = \sum_{n=0}^{\infty} B_n J_n(k_{L1} r)\cos(n\theta) e^{i(k_Z z - \omega t)} \tag{10}$$

$$[\psi_1]_r = \sum_{n=0}^{\infty} C_n J_{n+1}(k_{T1} r)\sin(n\theta) e^{i(k_Z z - \omega t)}$$

$$[\psi_1]_\theta = \sum_{n=0}^{\infty} -C_n J_{n+1}(k_{T1} r)\cos(n\theta) e^{i(k_Z z - \omega t)}$$

$$[\psi_1]_z = \sum_{n=0}^{\infty} D_n J_n(k_{T1} r)\sin(n\theta) e^{i(k_Z z - \omega t)}$$

$$\phi_2 = \sum_{n=0}^{\infty} [E_n J_n(k_{L2}r) + F_n Y_n(k_{L2}r)]\cos(n\theta)\, e^{i(k_Z z - \omega t)}$$

$$[\psi_2]_r = \sum_{n=0}^{\infty} [K_n J_{n+1}(k_{T2}r) + L_n Y_{n+1}(k_{T2}r)]\sin(n\theta)\, e^{i(k_Z z - \omega t)}$$

$$[\psi_2]_\theta = \sum_{n=0}^{\infty} [-K_{n+1} J_n(k_{T2}r) - L_n Y_{n+1}(k_{T2}r)]\cos(n\theta)\, e^{i(k_Z z - \omega t)}$$

$$[\psi_2]_z = \sum_{n=0}^{\infty} [M_n J_n(k_{T2}r) + N_n Y_n(k_{T2}r)]\sin(n\theta)\, e^{i(k_Z z - \omega t)}$$

where

$$k_{L_2}^2 = (\frac{\omega}{c_{L_2}})^2 - k_z^2 ;\; k_{T_2}^2 = (\frac{\omega}{c_{T_2}})^2 - k_z^2 \tag{11}$$

c_{L_2} and c_{T_2} are the compression and shear wave velocities in the cladding material, respectively. E_n, F_n, K_n, L_n, M_n, N_n are unknown coefficients.

Boundary Conditions

There are twelve boundary conditions at the core-cladding and matrix-cladding interfaces. The boundary conditions (continuity of stresses and displacement) at the matrix-cladding interface, $r = a$, are:

$$[\sigma_{r\theta}]_2 = [\sigma_{r\theta}]_3 ; \quad [\sigma_{rr}]_2 = [\sigma_{rr}]_3 ; \quad [\sigma_{rz}]_2 = [\sigma_{rz}]_3 \tag{12}$$
$$[u_r]_2 = [u_r]_3 ; \quad [u_\theta]_2 = [u_\theta]_3 ; \quad [u_z]_2 = [u_z]_3$$

At the core-cladding interface, $r = b$, the corresponding boundary conditions are:

$$[\sigma_{r\theta}]_1 = [\sigma_{r\theta}]_2 ; \quad [\sigma_{rr}]_1 = [\sigma_{rr}]_2 ; \quad [\sigma_{rz}]_1 = [\sigma_{rz}]_2 \tag{13}$$
$$[u_r]_1 = [u_r]_2 ; \quad [u_\theta]_1 = [u_\theta]_2 ; \quad [u_z]_1 = [u_z]_2$$

where expressions for the stress at any point can be derived from the determined displacement field. Inserting the potential functions from Eqs. (7) and (11) in Eqs. (13) and (14), results in the following system of twelve linear algebraic equations,

$$[D_n]\{T_n\} = \{Q_n\}, \tag{14}$$

where

$$\{T_n\} = [B_n \quad C_n \quad D_n \quad E_n \quad F_n \quad K_n \quad L_n \quad M_n \quad N_n \quad P_n \quad R_n \quad S_n]^T ; \tag{15}$$
$$\{Q_n\} = [b_1 \quad b_2 \quad b_3 \quad b_4 \quad b_5 \quad b_6 \quad b_7 \quad b_8 \quad b_9 \quad b_{10} \quad b_{11} \quad b_{12}]^T ;$$

$[D_n]$ is a 12×12 matrix with components designated as a_{ij}. Eq. (15) can be solved for unknown coefficients at any given value of normalized frequency ka.

For the case of incident compression waves, the resulting normalized far-field amplitude spectrum, which is called the form function, is obtained from the following equation [13],

$$f_\infty(\theta, K_2 a) = \sum_n (2/\sqrt{i\pi K_2 a})(-1)^n \varepsilon_n Q_n, \tag{16}$$

and for incident shear waves (of either $r-z$ or $r-\theta$ polarization) by

$$f_\infty(\theta, k_2 a) = \sum_n (2/\sqrt{i\pi k_2 a})(-1)^n \varepsilon_{sn} Q_n. \tag{17}$$

The parameter Q_n which is equal to one of the coefficients P_n, R_n or S_n depends on the type of the scattered wave, as defined in Eqs. (5), (6) and (7).

NUMERICAL RESULTS

To verify the mathematical model, form functions of an immersed copper clad-aluminum rod and a steel fiber encased in epoxy matrix are each calculated for some incident angles. Verification of the model is done by considering an isotropic cylinder covered by isotropic cladding. The form function is evaluated for a copper clad-aluminum rod immersed in water for two incident angles. The corresponding form functions shown in Fig. 2 are identical to those of Fig. 2, Ref. [13].
Verification of the model is also done by considering an isotropic cylinder encased in an isotropic matrix. The form function is evaluated for a steel fiber encased in epoxy matrix. The corresponding form functions shown in Fig. 3 are fully identical to those of Fig. 2, Ref. [13]. Using this model, form functions of an alumina (Al_2O_3) fiber-zirconia (ZrO_2) cladding encased in aluminum (AA520) matrix for two incident angles of 3° and 5° are presented in Fig. 4. Elastic properties for aluminum, copper, steel, epoxy, alumina (Al_2O_3), aluminum (AA520), zirconia (ZrO_2) and water were taken from Ref.'s [12], [13] and [15].

CONCLUSIONS

In this paper, a mathematical model for scattering of an obliquely incident plane acoustic wave from an isotropic clad rod encased in an isotropic matrix was developed. The isotropic matrix was modeled by decomposition of the displacement field into three potential functions. The displacement filed inside the isotropic clad-rod was formulated using Helmholtz decomposition technique. The boundary conditions were applied to determine the unknown scattering coefficients. Using this model, two special acoustic wave scattering problems were studied: a) an immersed isotropic cylinder covered by isotropic cladding and b) an encased isotropic cylinder and encased isotropic clad-rod. The form functions are identical to those reported in other references. The form function of an isotropic alumina (Al_2O_3) fiber covered by zirconia (ZrO_2) and encased in aluminum (AA520) matrix was calculated.

REFERENCES

1. R. M. White, J. Acoust. Soc. Am. 30, 771-785 (1958).
2. V. V. Tyutekin, J. Sov. Phys. Acoust. 5, 105-109 (1959).
3. Y. H. Pao and C. C. Mao, Diffraction of Elastic waves and dynamic stress concentrations (Crane, Russack, New York), (1973).
4. D. J. Jain and R. P. Kanwal, J. Appl. Phys. 50, 4067-4109 (1979).
5. A. N. Sinclair and R.C. Addison, J. Acoust. Soc. Am. 94, 1126-1135 (1993).
6. W. Huang, S. Brisuda, S. I. Rokhlin, Ultrasonics 33, 365-375 (1995)
7. W. Huang, S. I. Rokhlin, and Y. J. Wang, in Review of Progress in QNDE, edited by D. O. Thompson and D. E. Chimenti (Plenum, New York, 1994), Vol. 13, pp. 1367-1374.
8. W. Huang, S. I. Rokhlin, and Y. J. Wang, J. Acoust. Soc. Am. 97, 807-817 (1995).
9. P. H. Johnston, J. H. Williams, and G. Khanna, in Review of Progress in QNDE, edited by D. O. Thompson and D. E. Chimenti (New York, 1995), Vol. 13, pp. 1299-1306.
10. W. Huang, S. I. Rokhlin, and Y. J. Wang, J. Acoust. Soc. Am. 99(5), 2742-2754 (1996).
11. F. Honarvar and A. N. Sinclair, J. Acoust. Soc. Am. 100(1), 57-63 (1996).
12. F. Honarvar and A. N. Sinclair, J. Acoust. Soc. Am. 102(1), 41-47 (1997).
13. Y. Fan, A. N. Sinclair and F. Honarvar, J. Acoust. Soc. Am. 106 (3), 1-8 (1999).
14. P. Beattie, R. C. Chivers, and L. W. Anson, J. Acoust. Soc. Am. 94, 3421-3427 (1993).
15. L. Cai,, J. Acoust. Soc. Am. 115(2), 515-522 (2004).

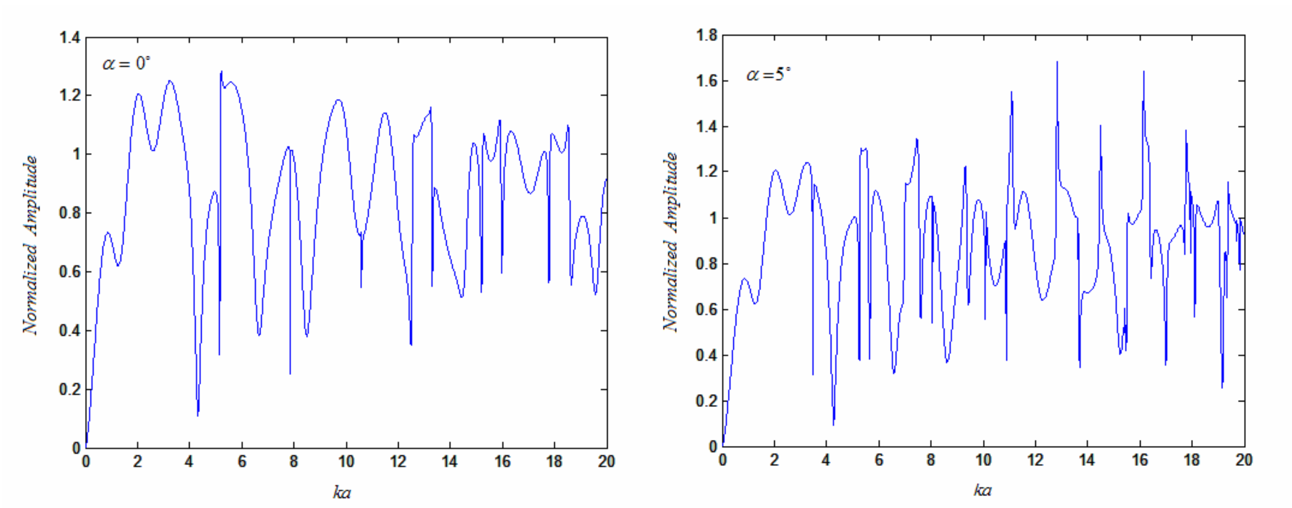

Fig. 2- Copper clad-aluminum rod form functions at incident angles $\alpha = 0^\circ, 5^\circ$.

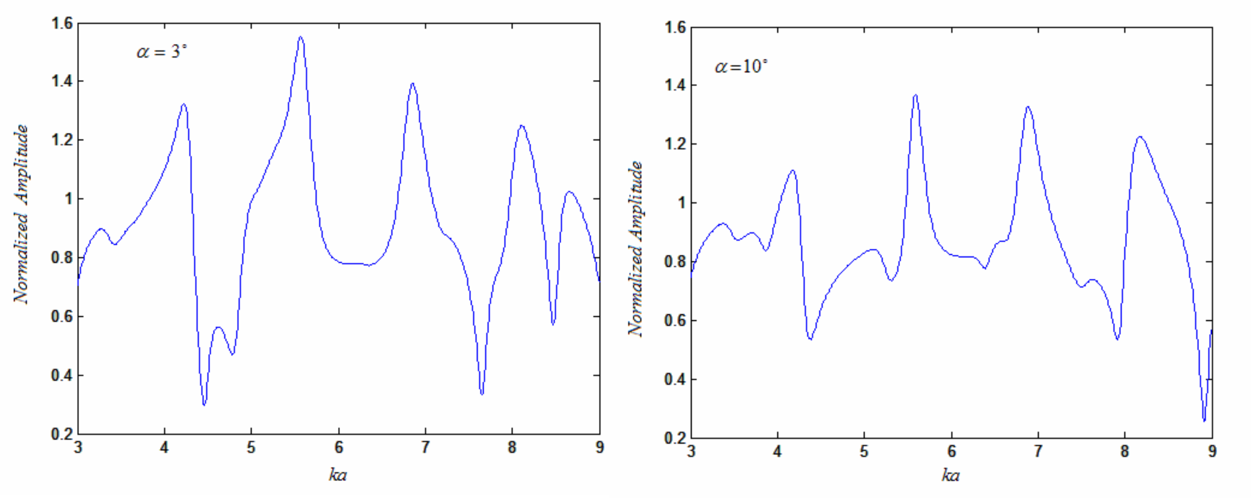

Fig. 3- Form functions of steel fiber encased in epoxy at incident angles $\alpha = 3^\circ, 10.^\circ$.

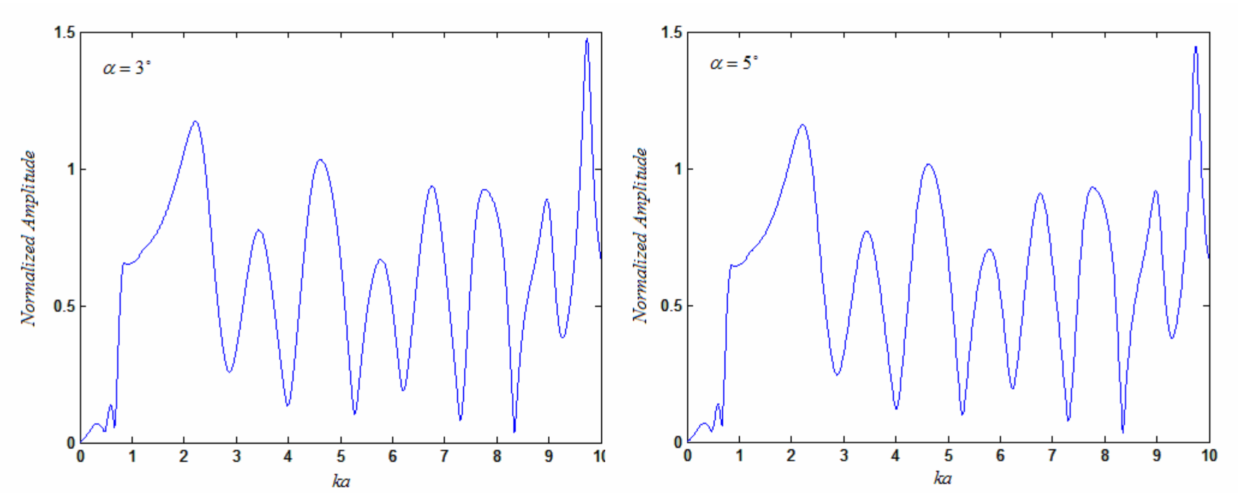

Fig. 4- Form functions for alumina fiber-zirconia cladding encased in aluminum matrix at incident angles $\alpha = 3^\circ, 5^\circ$.